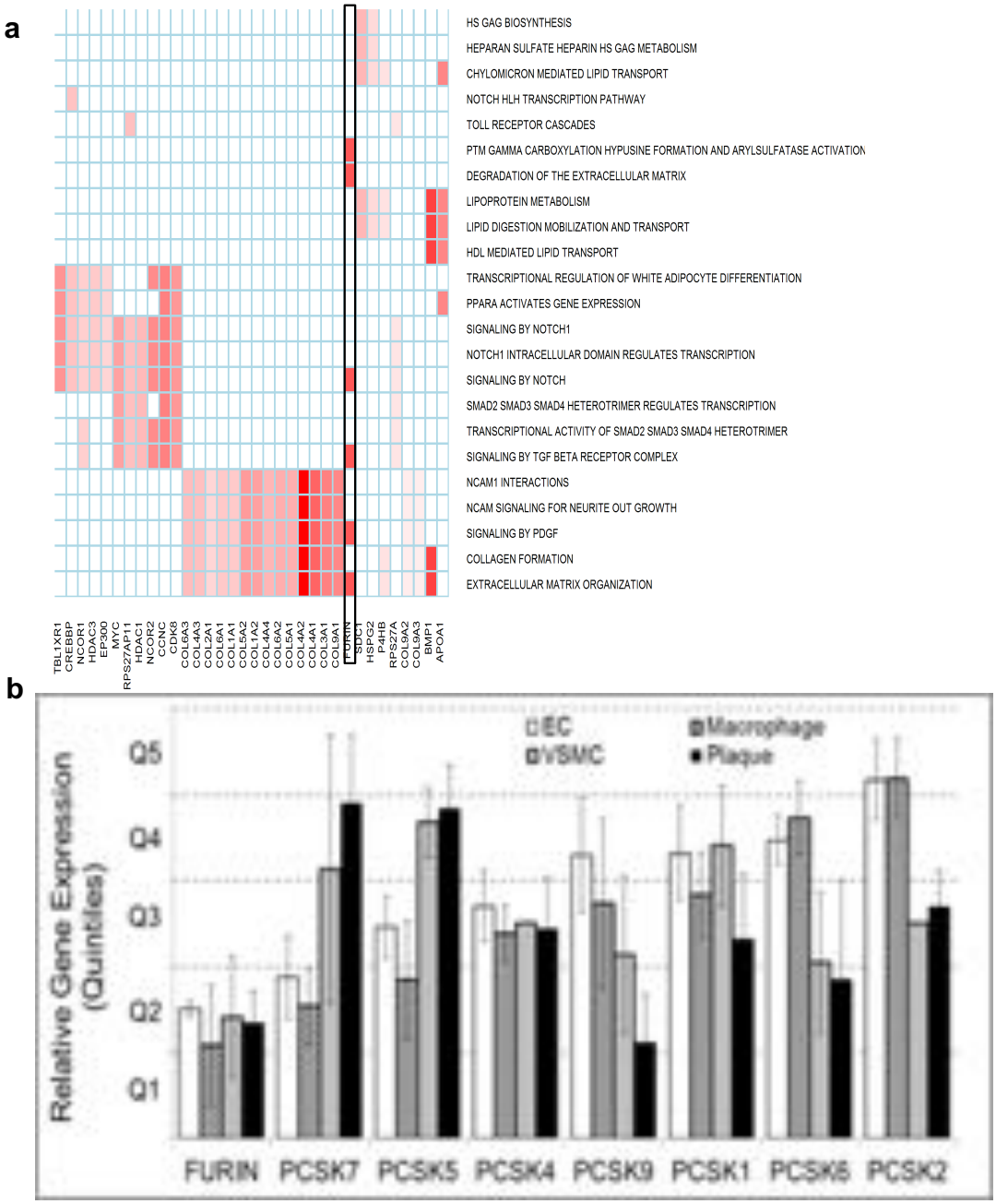

Figure 1: Genetic and genomic evidence for the association of *FURIN* with CAD. (a) Heatmap representing genes that are common members of biological pathways significantly associated with CAD[4]. The results for FURIN are highlighted in the black-bordered rectangle. Heatmap is color-coded by the negative logarithm of the CAD-association p-values for the respective genes. **(b)** Expression of FURIN in genome-scale expression datasets in Gene Expression Omnibus. Expression of FURIN and other PCSKs were quantified in 570 samples encompassing vascular endothelial cells (EC), vascular smooth muscle cells (VSMC), monocyte/macrophages (Macrophage) and human atherosclerotic plaques (Plaque). To allow comparisons between disparate experiments, gene expression levels were converted to quantiles (quintiles) with quintile 1 (Q1) representing the top 20% expressed genes.

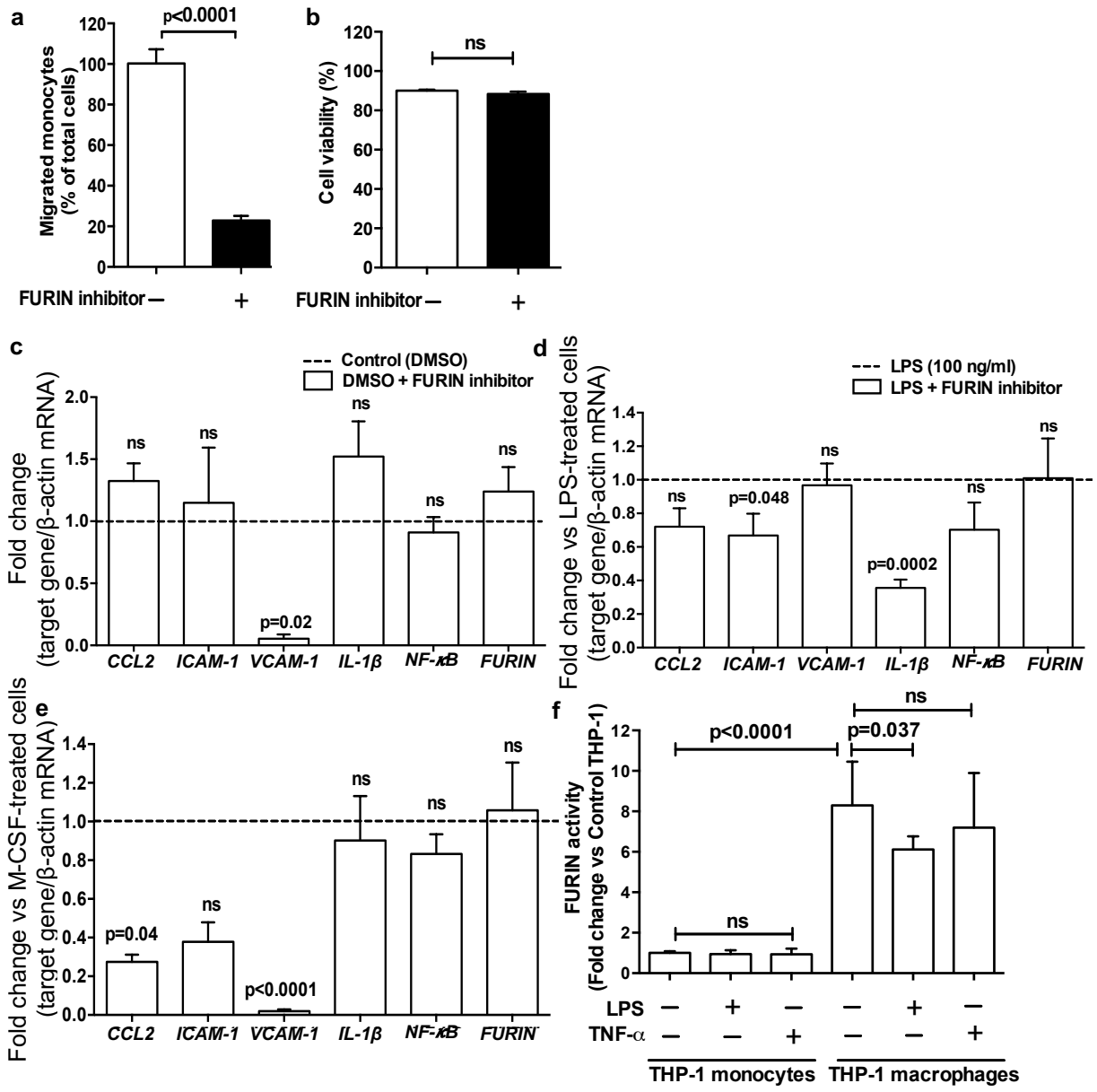

Figure 2: FURIN inhibition decreases monocyte migration and inflammatory gene expression *in vitro*. (a) Activated human THP-1 monocytes were subjected to trans-well migration assays. In the presence of the FURIN inhibitor Dec-RVKR-CMK, a significantly lower number of monocytes migrated to the chemo-attractant M-CSF, and **(b)**, the lower number of transmigrated monocytes did not result from increased cell death. **(c)** Lower *VCAM-1* expression level in FURIN inhibitor treated monocytes. **(d)** *ICAM-1* and *IL-1β* transcription is significantly reduced in FURIN inhibitor treated monocytes upon LPS stimulation. **(e)** *CCL2* and *VCAM-1* transcription is significantly reduced in FURIN inhibitor treated M-CSF derived macrophages. **(f)** FURIN activity is significantly decreased in LPS-treated macrophages. Data represent mean ± SEM of 3 independent experiments performed in triplicate. The dotted lines in **(c)**, **(d)** and **(e)** represent control values. Data in **a**,**b** and **f** are normally distributed, and p-values were assessed using Student's T-tests. Data in **c**-**e** were not normally distributed, and Kruskal-Wallis ANOVA tests were used.

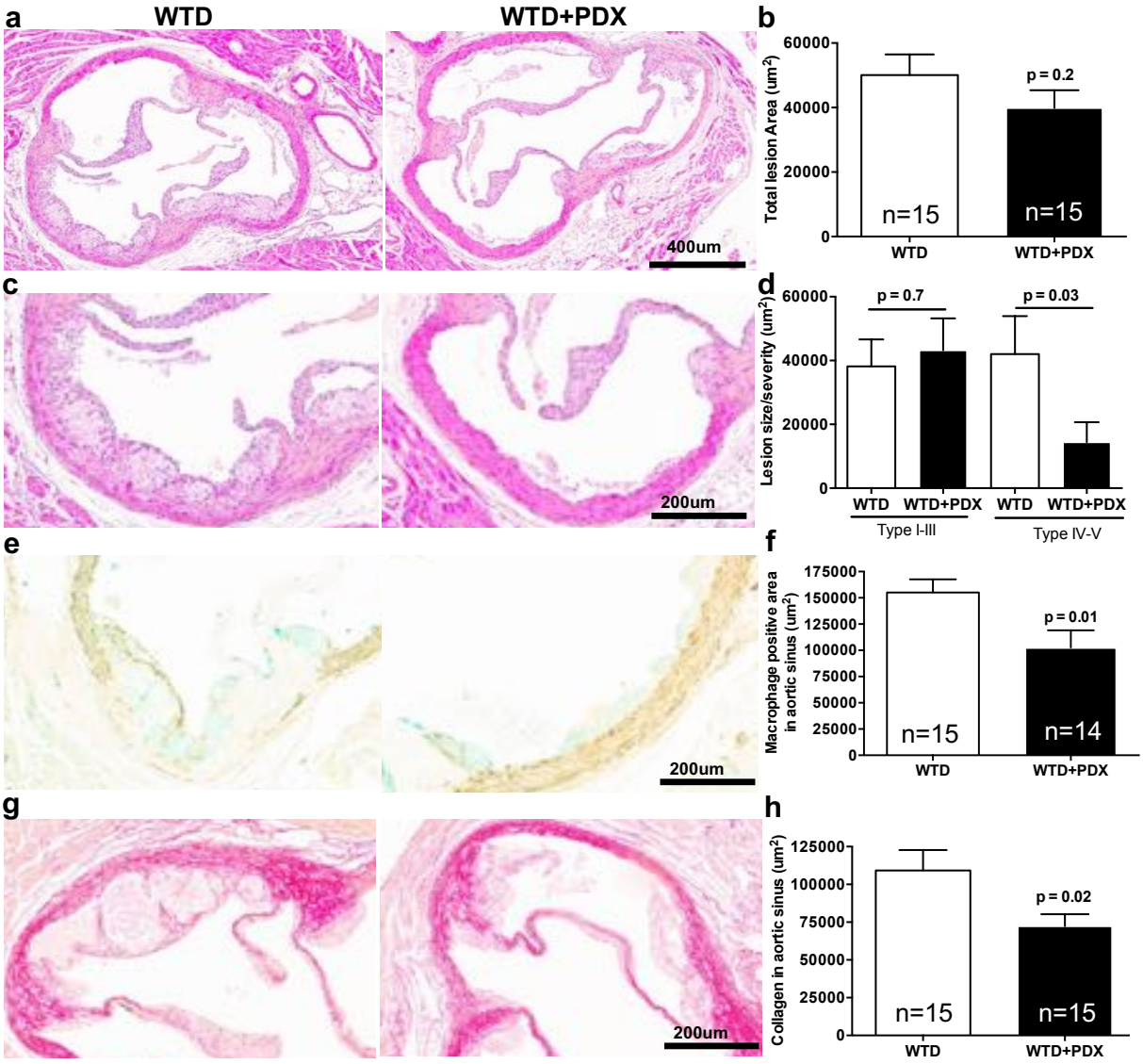

Figure 3: Lower lesion complexity and severe atherosclerotic lesion size in FURIN inhibitor treated mice. (a) Representative photomicrographs of aortic sinus after histological staining with hematoxylin-phloxine-saffron (200x). **(b)** A trend toward lower aortic sinus lesion area in FURIN inhibitor treated mice. **(c)** Representative photomicrographs of lesion severity in aortic sinus after histological staining with hematoxylin-phloxine-saffron (100x). **(d)** Significantly lower severe lesion area (type IV and V) in FURIN inhibitor treated mice. **(e)** Representative photomicrographs of macrophages (green) in aortic sinus (100x). **(f)** Significantly lower lesional macrophage area in FURIN inhibitor treated mice. **(g)** Representative photomicrographs of aortic root after histological staining with picrosirius red for collagen (100x). **(h)** Significantly lower collagen area in lesions of FURIN inhibitor treated mice. Groups are abbreviated as: *Ldlr*$^{-/-}$ mice fed Western type diet injected with PBS (WTD); *Ldlr*$^{-/-}$ mice fed Western type diet injected with the α-1-PDX FURIN inhibitor (WTD+PDX). All mice are male. Values represent mean ± SEM. Data in **f** and **h** are normally distributed, and p-values were assessed using Student's T-tests. Data in **b** and **d** were not normally distributed, and Mann-Whitney tests were used.

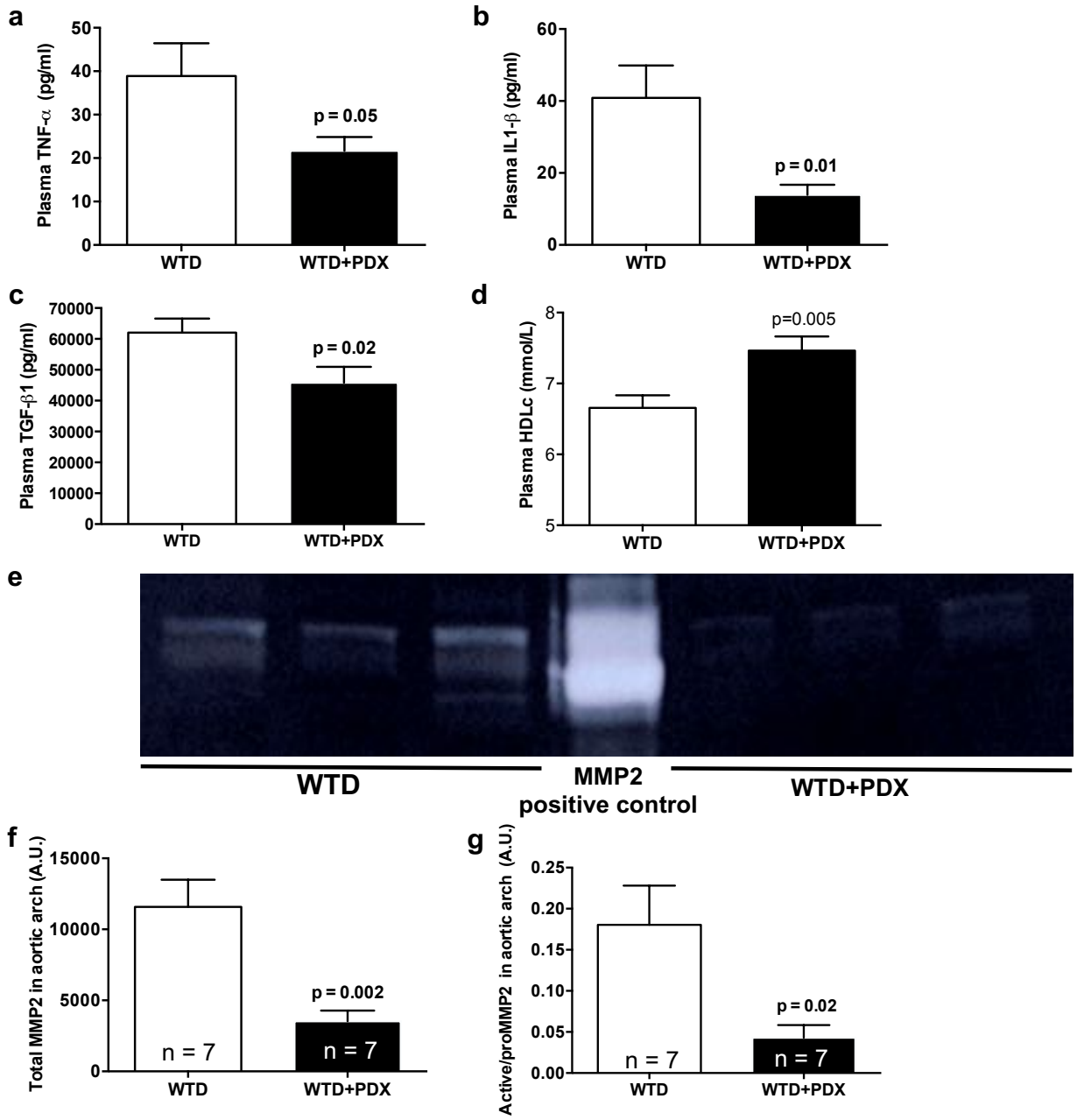

Figure 4: Lower plasma inflammatory markers, elevated plasma HDL cholesterol and lower MMP2 expression in aorta of FURIN inhibitor treated mice. Lower plasma levels of **(a)** TNF-α, **(b)** IL1-β, **(c)** TGF-β1, and **(d)** elevated plasma HDL cholesterol levels in FURIN inhibitor treated mice. n=14-16 for all analyses. **(e)** Gelatin zymography in the aortic arch showing both the pro and active forms of MMP2. **(f)** Total MMP2 expression levels are significantly lower in the aortic arch of FURIN inhibitor treated mice. **(g)** Significantly lower active MMP2/proMMP2 expression in the aortic arch of FURIN inhibitor treated mice. Groups are abbreviated as: *Ldlr*$^{-/-}$ mice fed Western type diet injected with PBS (WTD); *Ldlr*$^{-/-}$ mice fed Western type diet injected with the α-1-PDX FURIN inhibitor (WTD+PDX). A.U.= Arbitrary Units. Values represent mean ± SEM. All mice are male. Data in **a**-**f** are normally distributed, and p-values were assessed using Student's T-tests. Data in **g** are not normally distributed, and Mann-Whitney test was performed.

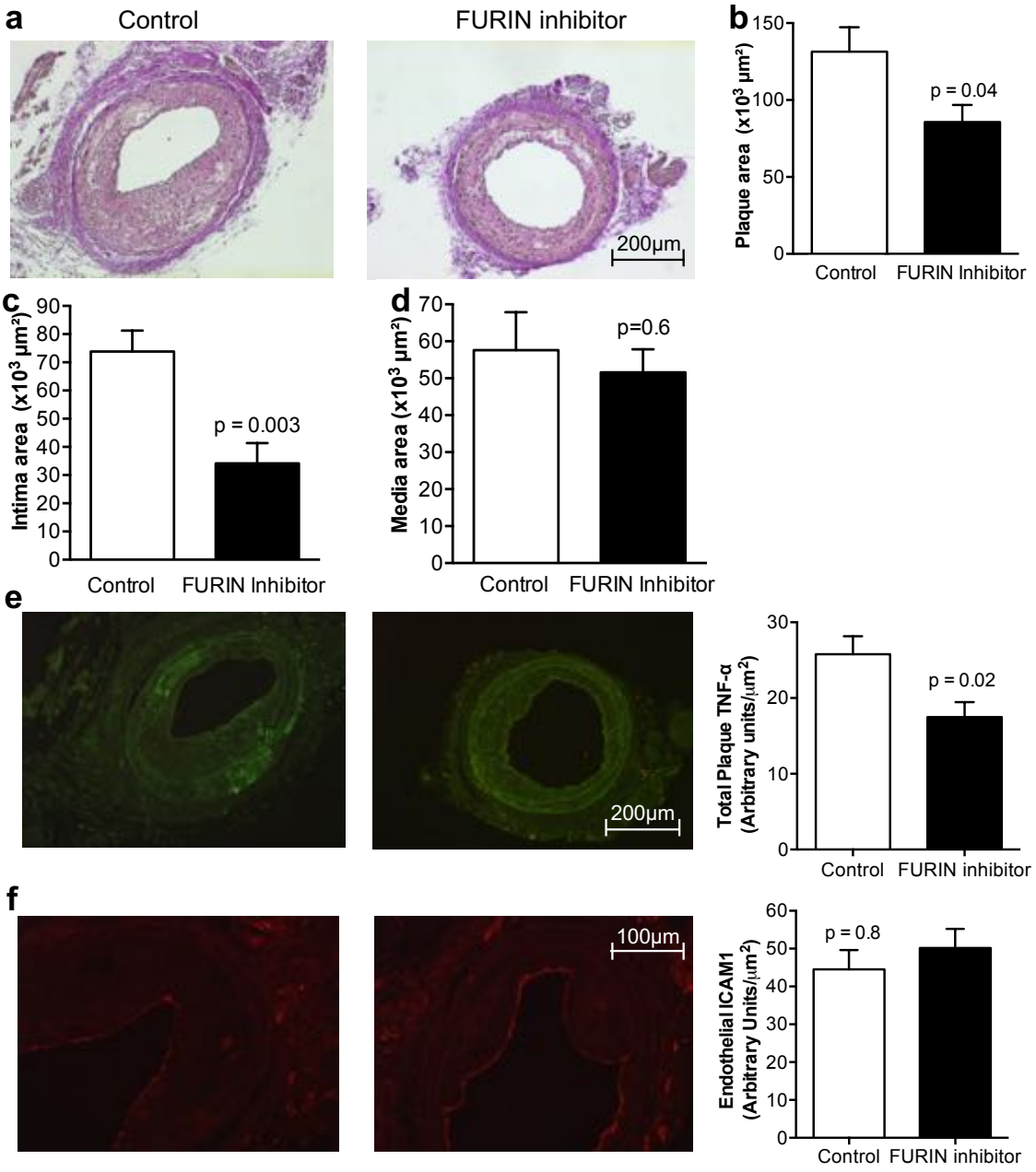

Figure 5: FURIN inhibition reduces neointimal plaque formation and inflammation in a wire injury model of atherosclerosis. Male *Apoe*$^{-/-}$ mice were fed a high-fat diet, treated with vehicle (DMSO) or FURIN Inhibitor α-1-PDX and were subjected to wire injury of the common carotid artery. **(a)** Representative photomicrographs of pentachrome-stained sections 2 weeks after injury, **(b)** Significantly lower plaque area, **(c)** Significantly lower neointima area, and **(d)** Unchanged media area in FURIN inhibitor treated mice**. (e)** Significantly decreased vascular inflammatory cytokine TNF-α levels (stained in green), and **(f)** Unchanged endothelial adhesion molecule ICAM1 levels (stained in red) in FURIN inhibitor treated mice. Groups are abbreviated as: *Apoe*$^{-/-}$ mice (Control); Ap*oe*$^{-/-}$ mice administered the FURIN inhibitor α-1-PDX (FURIN inhibitor). n=6 per group. Values represent mean ± SEM. Data in **a-e** are normally distributed, and p-values were assessed using Student's T-tests. Data in **f** was not normally distributed and a Mann-Whitney test was used.

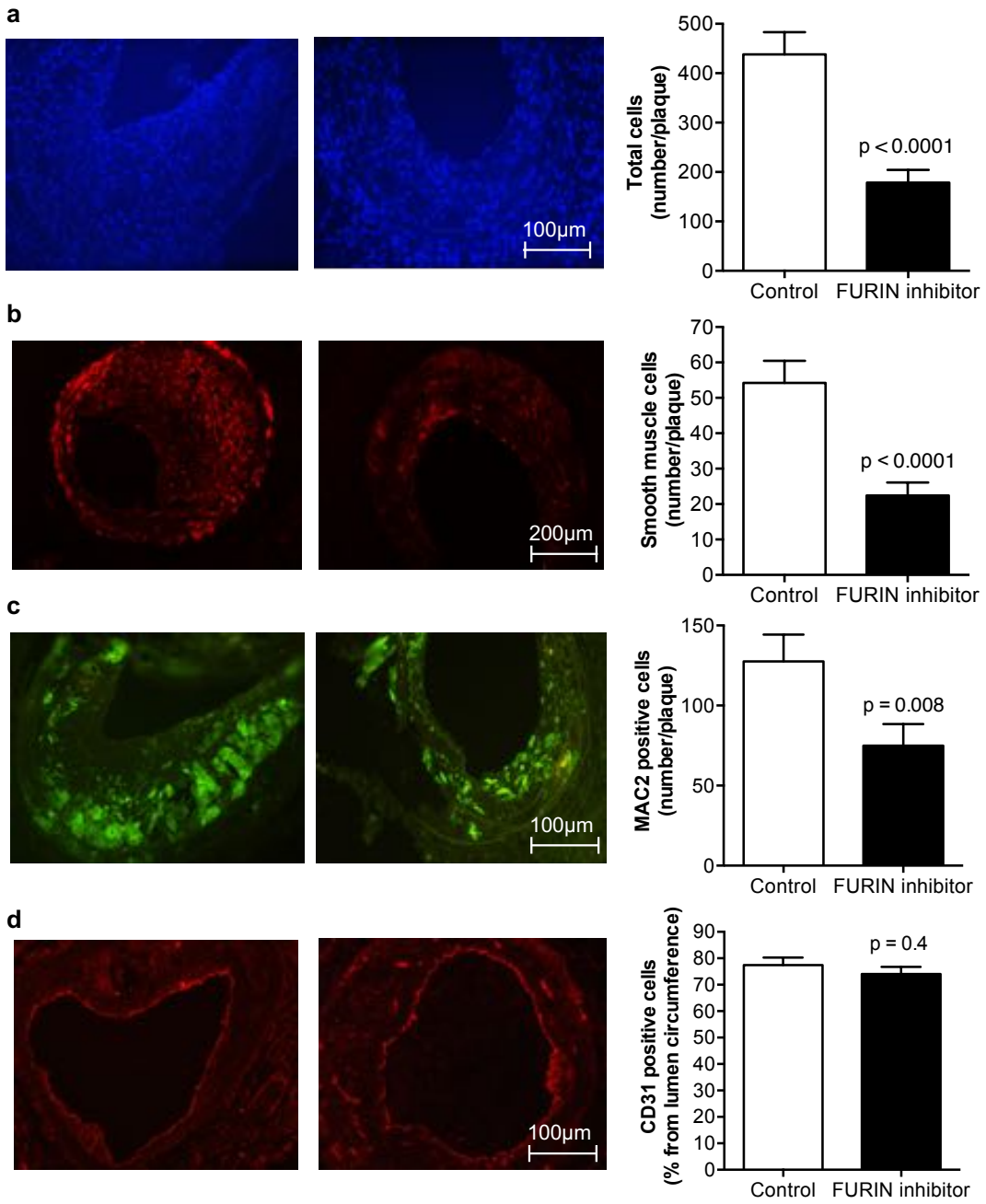

Figure 6: FURIN inhibition reduces plaque complexity in a wire injury model of atherosclerosis. Male *Apoe*$^{-/-}$ mice were fed a high-fat diet, treated with vehicle (control) or FURIN Inhibitor α-1-PDX and subjected to wire-induced injury of the common carotid artery. **(a)** The total number of cells, **(b)** the number of smooth muscle cells, and **(c)** the number of MAC2 positive macrophages per plaque were all significantly lower in FURIN inhibitor treated mice. **(d)** No changes in CD31^{+} endothelial cell numbers were observed. Groups are abbreviated as: *Apoe*$^{-/-}$ mice (Control); Ap*oe*$^{-/-}$ mice administered the FURIN inhibitor α-1-PDX (FURIN inhibitor). n=6 per group. Values represent mean ± SEM. Data in **a**-**c** are not normally distributed, and p-values were assessed using Mann-Whitney tests. Data in **d** is normally distributed, and Student's T-test was used.

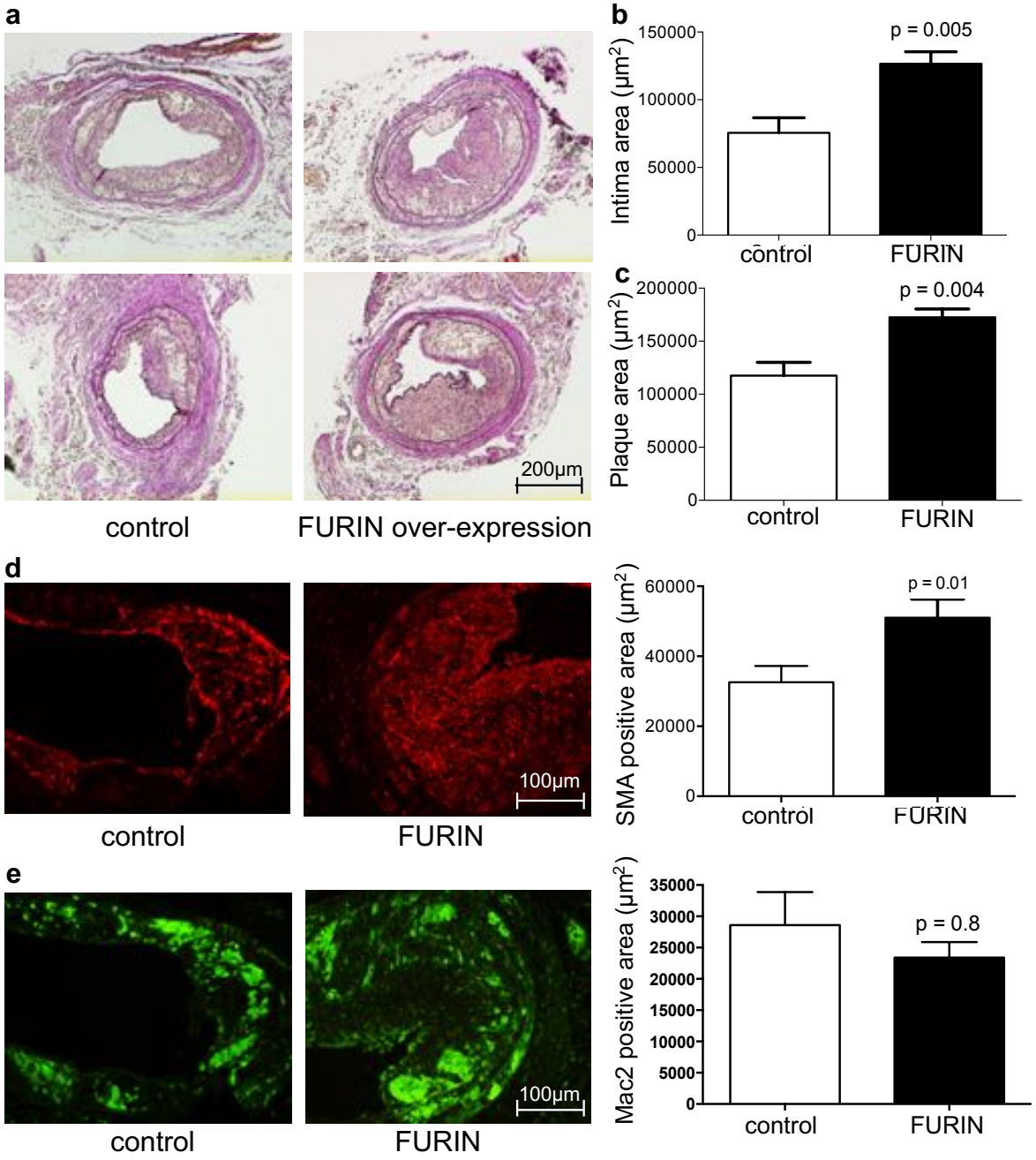

Figure 7: FURIN over-expression increases neointimal plaque formation in a wire injury model of atherosclerosis. Male *Apoe*$^{-/-}$ mice were fed a western-type diet, subjected to wire-induced injury of the common carotid artery, and treated with vehicle (n=5) or purified FURIN protein (n=6). **(a)** Representative photomicrographs of pentachrome-stained sections at 2 weeks after injury, and **(b)** significantly higher neointima and **(c)** plaque area in FURIN protein injected mice**. (d)** Significantly increased smooth muscle cell area (stained in red), and **(e)** no change in macrophage area (stained in green) in the lesions of FURIN over-expressing mice. Groups are abbreviated as: *Apoe*$^{-/-}$ mice (Control); Apo*e*$^{-/-}$ mice administered purified FURIN protein (FURIN). Values represent mean ± SEM. Data in **a**-**d** are normally distributed, and p-values were assessed using Student's T-tests. Data in **e** is not normally distributed, and the Mann-Whitney test was used.

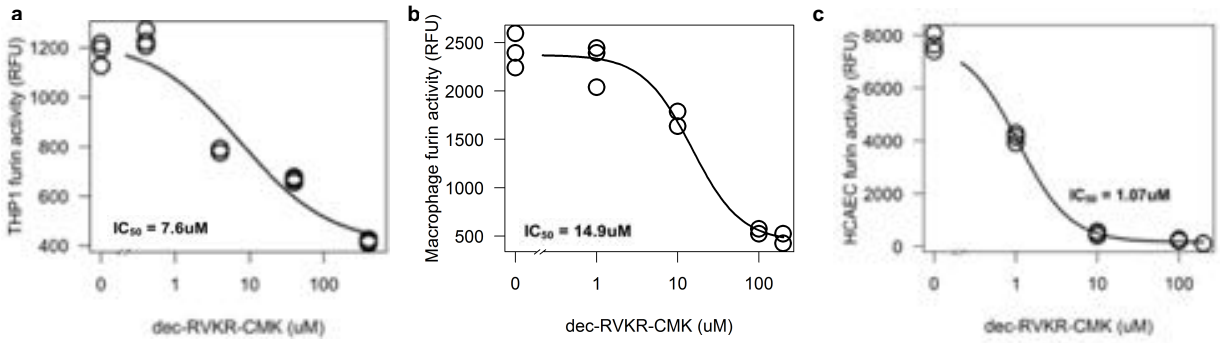

Supplementary figure 1: Dose response curve for the FURIN inhibitor Decanoyl-RVKR-CMK. Dose response curve in **(a)** THP1 human monocyte cells, **(b)** in THP1-derived macrophages, and **(c)** in human coronary artery endothelial cells. Dose-response curves were generated via the *drc* software in R, based on a 4-parameter log-logistic model.

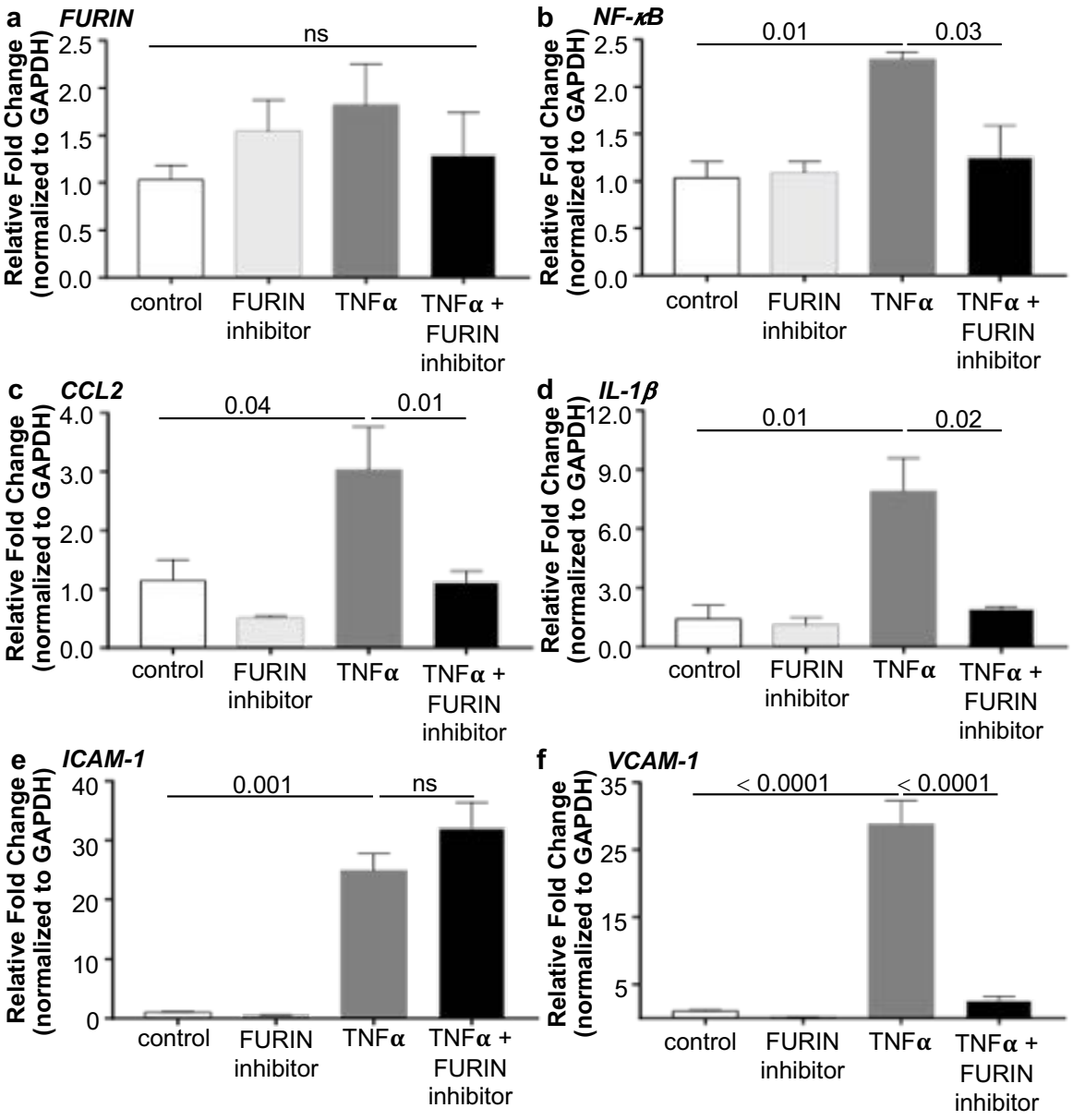

Supplementary figure 2: FURIN inhibition reduces vascular endothelial cell cytokine, chemokine and inflammatory gene expression *in vitro*. (a) *FURIN* gene expression is not changed, **(b)** *NF-κB*, **(c)** *CCL2*, and **(d)** *IL-1β* expression levels are significantly decreased, **(e)** *ICAM-1* levels are not changed, and **(f)** *VCAM-1* expression levels are significantly decreased in TNFα-stimulated, FURIN inhibitor (Dec-RVKR-CMK) treated human aortic endothelial cells. Values represent the mean ± SEM. Data are normally distributed, and p-values generated by one-way ANOVA followed by Tukey's post hoc test.

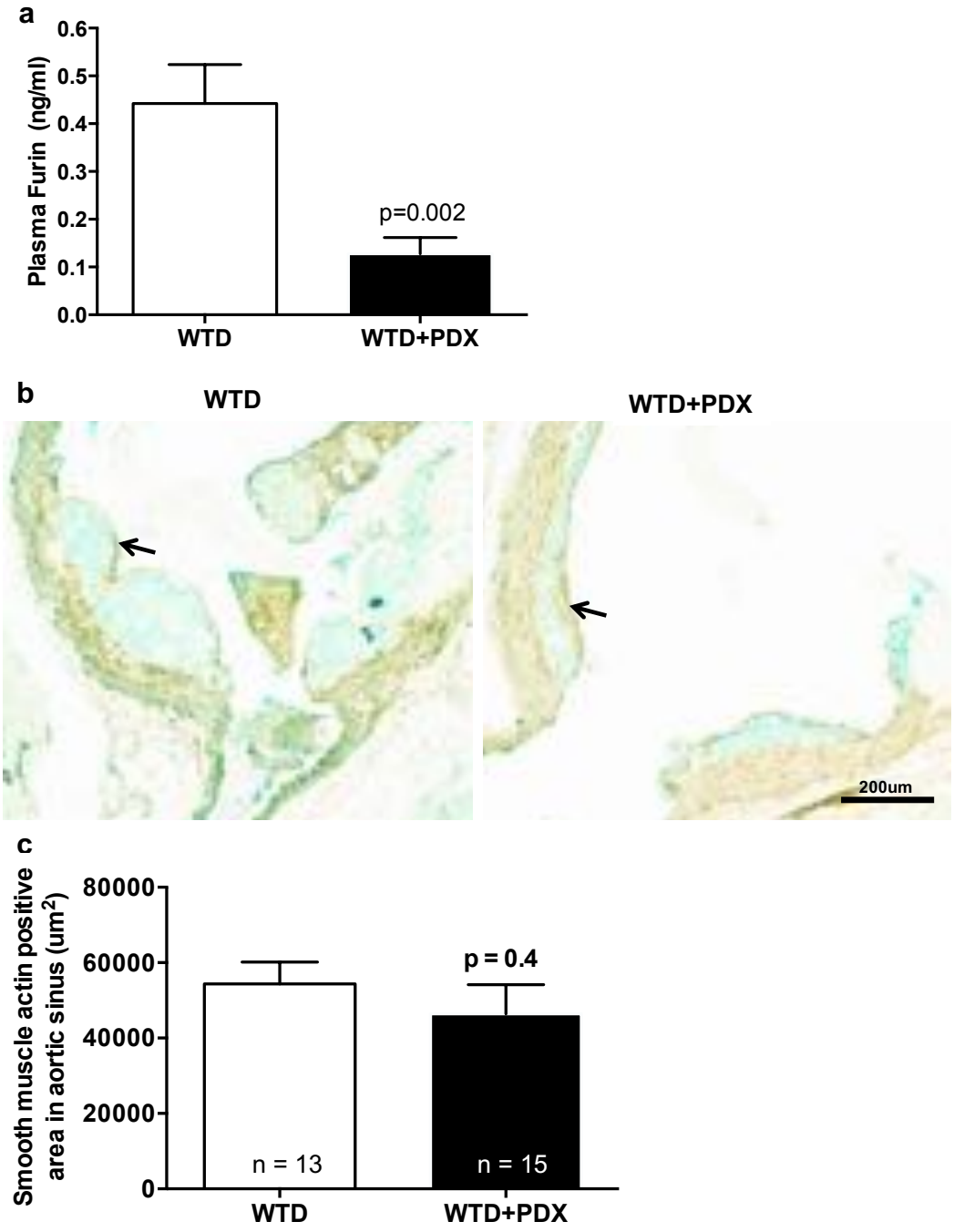

Supplementary figure 3: FURIN inhibitor treatment reduces plasma FURIN levels and does not affect smooth muscle actin expression in the aorta. (a) Plasma FURIN levels are significantly reduced in α-1-PDX FURIN inhibitor treated western type diet fed *Ldlr*$^{-/-}$ mice. **(b)** Representative photomicrographs of the aortic root after histological staining with smooth muscle actin (SMA, brown), and **(c)** No change in SMA expression in the aortic sinus. Groups are abbreviated as: *Ldlr*$^{-/-}$ mice fed Western type diet injected with PBS (WTD); *Ldlr*$^{-/-}$ mice fed Western type diet injected with the α-1-PDX FURIN inhibitor (WTD+PDX). All mice are male. Values are mean ± SEM. Data are normally distributed, and p-values were assessed using Student's T-tests.

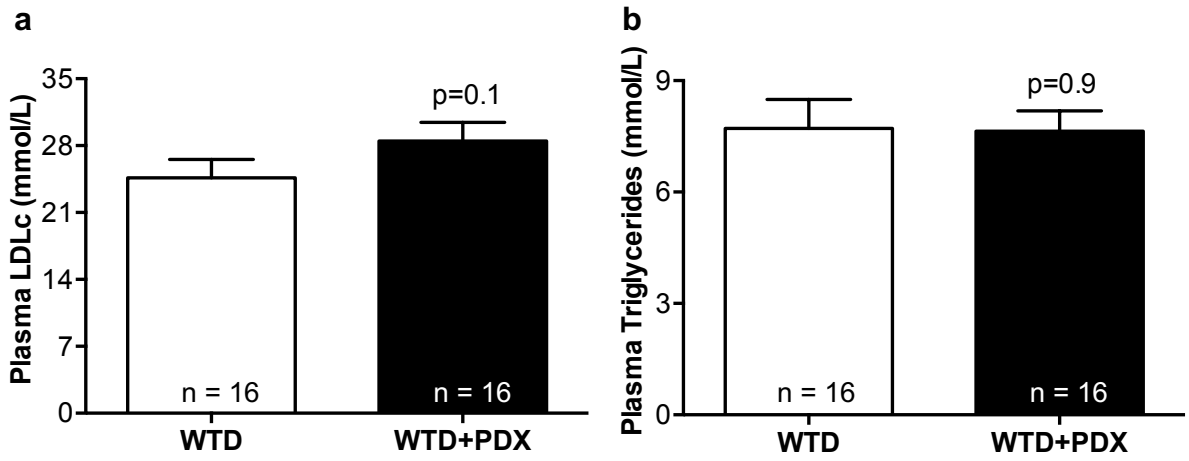

Supplementary figure 4: No changes in plasma triglycerides and LDL cholesterol levels in FURIN inhibitor treated mice. (a) Plasma LDL cholesterol levels, and **(b)** Plasma triglyceride levels are unchanged in FURIN inhibitor treated mice. Groups are abbreviated as: *Ldlr*$^{-/-}$ mice fed Western type diet injected with PBS (WTD); *Ldlr*$^{-/-}$ mice fed Western type diet injected with the α-1-PDX FURIN inhibitor (WTD+PDX). All mice are male. Values represent the mean ± SEM. Data are normally distributed, and p-values were assessed using Student's T-tests.

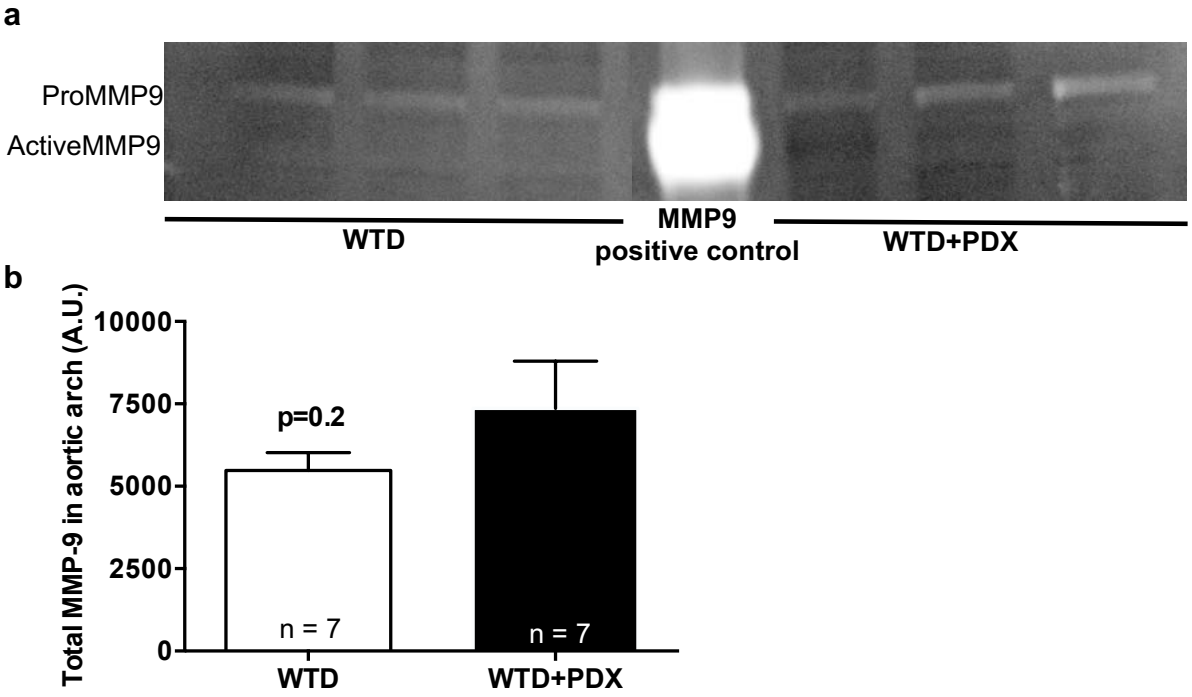

Supplementary figure 5: FURIN inhibition does not affect MMP9 expression in the aorta. (a) Gelatin zymography in the aortic arch, and **(b)** Quantification of total MMP9 expression in the aortic arch. Groups are abbreviated as: *Ldlr*$^{-/-}$ mice fed Western type diet injected with PBS (WTD); *Ldlr*$^{-/-}$ mice fed Western type diet injected with the α-1-PDX FURIN inhibitor (WTD+PDX). A.U.= Arbitrary Units. All mice are male. Values represent the mean ± SEM. Data are normally distributed, and p-values were assessed using Student's T-tests.

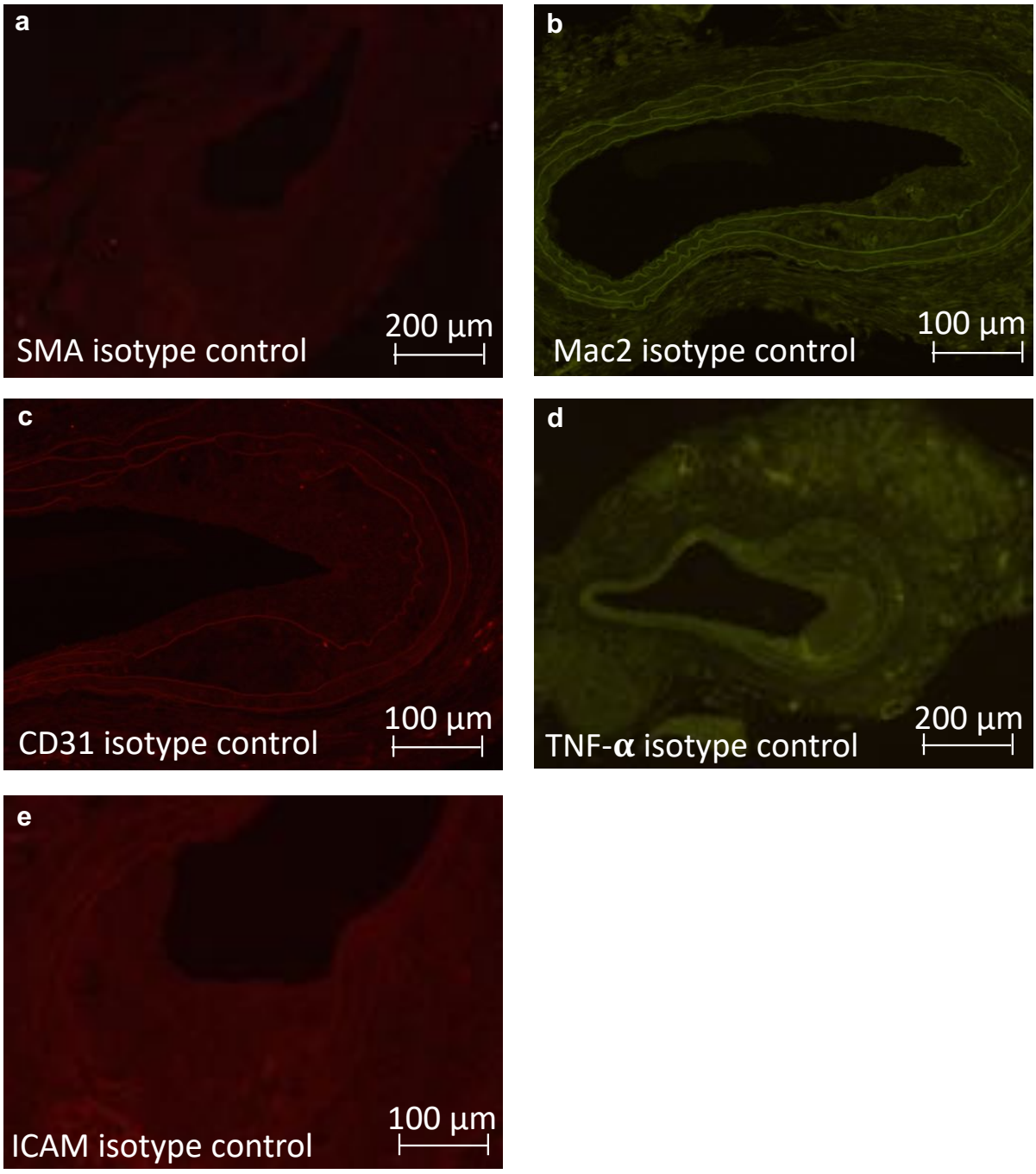

Supplementary figure 6: Isotype-specific immunoglobulin negative controls. (a) Isotype control for the anti-smooth muscle actin (SMA) antibody, **(b)** Isotype control for the anti-MAC2 macrophage antibody, **(c)** Isotype control for the anti-CD31 endothelial cell antibody, **(d)** Isotype control for the anti-TNF-α antibody, and **(e)** Isotype control for the anti-ICAM1 antibody in adjacent sections from wild-type control mice.